Communication

Compact 5G MIMO Mobile Phone Antennas With Tightly Arranged Orthogonal-Mode Pairs

Libin Sun, Haigang Feng, Yue Li, and Zhijun Zhang

***Abstract*— In this communication, the novel compact tightly arranged pairs are employed to form a 4 × 4 multiple-input-multiple-output (MIMO) system and an 8 × 8 MIMO system operating at 3.4–3.6 GHz for fifth-generation (5G) mobile phones. Each tightly arranged pair is composed of a bent monopole and an edge-fed dipole with a compact size of 7 × 12 mm^2. The orthogonal-mode method is presented to mitigate the mutual coupling of the tightly arranged pairs without any external decoupling structure. With the help of the orthogonal mode, isolation performances across the desired band of the 4 × 4 MIMO system and the 8 × 8 MIMO system are better than 20 and 17 dB, respectively, with the elements closely spaced. The measured efficiencies are 51.7%–84.5%/49%–72.9%, and the measured envelope correlation coefficients are less than 0.06/0.07 for the 4 × 4/8 × 8 MIMO system. The proposed MIMO systems provide a promising solution to compact 5G MIMO mobile phone antennas with good isolation and diversity performance.**

***Index Terms*— Decoupling, fifth generation (5G), mobile antennas, multiple input multiple output (MIMO), orthogonal mode, tightly arranged pair.**

I. Introduction

With the increasing demand of the quality of mobile communication, the fifth-generation (5G) mobile communication technology provides a promising solution to high communication rate, low time delay, massive connection density, and high communication capacity. To meet the aims of 5G mobile communication, a multiple-input-multiple-output (MIMO) technology has been developed for increasing the channel capacity of the communication system effectively in rich scattering environments. In the World Radiocommunication Conference 2015, the 3.5 GHz (3.4–3.6 GHz) band has become one of the 5G mobile phone frequency spectrums [1]. Recently, several papers have focused on the MIMO mobile phone antennas in the 5G frequency band [2]–[11]. However, with the limited region of mobile phones, it is a challenging task to integrate more antennas in a mobile phone with good isolation and low envelope correlation coefficient (ECC) [12].

There are several ways to mitigate the mutual coupling between two closely spaced antennas. The first method is adding a new coupling path to cancel out the primary coupling between two antennas, and the typical forms are the neutralization strip or decoupling element [13]–[15]. However, there is no intuitionistic design guideline for this method and it is difficult for a wideband mutual coupling reduction. The second way for decoupling is blocking up the coupling path by a defected ground structure or ground slits [16], [17]. Third, a matching network is an effective way to mitigate the mutual coupling but the bandwidth of this way is narrow [18]. The fourth way is the orthogonal mode, which is a natural decoupling technology without any additional structure. In [19] and [20], a good isolation and decoupling bandwidth have been obtained by orthogonal polarization. However, the size is too large for good application in a size-limited mobile phone.

There are several studies focusing on the compactness of the 5G MIMO antenna system, and a dual antenna pair is proposed to integrate two antennas closely with a good isolation for the aim of compactness [4]–[9]. In [4], a dual antenna pair with open-slot structure has been presented, and 10 dB isolation is achieved with the help of neutralization strip. A compact building block with two asymmetrically mirrored gap-coupled loop antennas is used in [5] and [6], and the compact building block is mounted along two opposite sides of the system ground plane. Coupling gap is used to block the surface currents, thus the isolation of better than 10 dB is obtained. In [7], an orthogonal-polarized loop structure has been investigated with 12 dB isolation. An orthogonal-mode pair has been proposed with 10 dB isolation recently in [8], but the ground clearance is as large as 12 mm. In [9], a pair of dual-band folded monopole has been presented, and a short neutral line is utilized for decoupling between two closely spaced monopoles.

In this communication, the compact tightly arranged orthogonal-mode pairs are employed to form a 4 × 4 MIMO system and an 8 × 8 MIMO system. The tightly arranged pair that has a compact size of 7 × 12 mm^2 is composed of a bent monopole and an edge-fed dipole. The antenna is mounted along the edge of the ground, and only 1 mm ground clearance is needed. Arranging two such tightly arranged pairs along each long edges of the ground plane, a 4 × 4 MIMO system is achieved. The 8 × 8 MIMO system can be obtained by disposing two such four-antenna systems at the up and down sides of the long edges. Different from the decoupling mechanism in [4]–[6], the orthogonal-mode method is presented in this communication to achieve a high isolation without any external decoupling structure. The isolation across the desired band of the 4 × 4 MIMO system and the 8 × 8 MIMO system is better than 20 and 17 dB, respectively, which is much better than the 5G mobile phone MIMO systems that have been proposed in [2]–[11]. The measured efficiencies of the 4 × 4/8 × 8 MIMO system are better than 51.7%/49% and 74.7%/61.6% when fed through port 1 (dipole mode) and port 2 (monopole mode), and the measured ECCs of all antenna elements are better than 0.06/0.07 for the 4 × 4/8 × 8 MIMO system. As far as the authors are concerned, it is the best isolation performance of a compact 5G MIMO smartphone antenna system with a desirable efficiency and ECC performance.

II. Four-Antenna MIMO System

A. Antenna Configuration of the 4 × 4 MIMO System

The 4 × 4 MIMO system composed of two tightly arranged pairs is illustrated in Fig. 1. A metal ground (150 × 73 mm^2) with only 1 mm clearance is printed on the back side of the FR-4

Manuscript received December 21, 2017; revised May 2, 2018; accepted August 2, 2018. Date of publication August 10, 2018; date of current version October 29, 2018. This work was supported by the National Natural Science Foundation of China under Contract 61525104. *(Corresponding author: Zhijun Zhang.)*

L. Sun, Y. Li, and Z. Zhang are with the Beijing National Research Center for Information Science and Technology, Tsinghua University, Beijing 100084, China (e-mail: zjzh@tsinghua.edu.cn).

H. Feng is with the Graduate School at Shenzhen, Tsinghua University, Shenzhen 518055, China (e-mail: feng.haigang@sz.tsinghua.edu.cn).

Color versions of one or more of the figures in this communication are available online at http://ieeexplore.ieee.org.

Digital Object Identifier 10.1109/TAP.2018.2864674

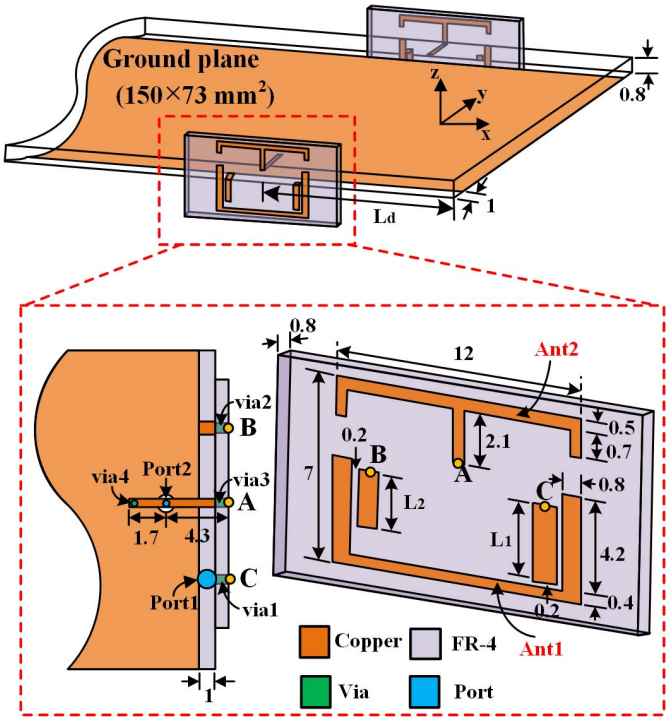

Fig. 1. Geometry of the 4 × 4 MIMO system composed of two tightly arranged dual antenna pairs, unit all in millimeters. Detailed dimensions: L_1 = 3 mm, L_2 = 2.45 mm, and L_d = 30 mm.

board ($\varepsilon_r = 4.4$, $\tan\delta = 0.02$), and the volume of the FR-4 board is 150 × 75 × 0.8 mm^3. Two small side FR-4 boards with a size of 20 × 8 × 0.8 mm^3 are mounted along the left and right sides of the ground plane. The tightly arranged pairs are printed on the outside of the side boards. The detailed structure of the tightly arranged pair is illustrated in the red dashed square as shown in Fig. 1. The tightly arranged pair that has a compact size of 12 × 7 mm^2 is composed of an edge-fed dipole (Ant1) and a bent T-shape monopole (Ant2). The size of Ant1 and Ant2 is 12 × 4.6 mm^2 and 12 × 2.6 mm^2, respectively. The edge-fed dipole (Ant1) is fed through port 1, and a via (via1) is drilled in the sideboard to excite the dipole through point C. A grounded strip that is added to keep the structure symmetric is connected to the ground plane through point B and via 2. It should be noted that the orthogonal mode will be deteriorated without the grounded strip. The monopole (Ant2) is fed through port 2, and via 3 is drilled in the sideboard to excite the monopole through point A. Port 2 is shorted through via 4 by a 1.7 mm strip, which can be equivalent to a shunt inductance to improve the impendence match of Ant2. The structure is simulated and optimized by a high-frequency structure simulator 15.0 software.

B. Decoupling Analysis

To describe the decoupling mechanism of the tightly arranged dual antenna pair, the vector current distributions are illustrated in Fig. 2. When port 1 (dipole mode) is excited and port 2 (monopole mode) is terminated to 50 Ω, the dipole (Ant1) is excited with current distributing along the *x*-axis as shown in Fig. 2(a). The current direction of the monopole (Ant2) distributes along the *z*-axis when port 2 is excited and port 1 is terminated to 50 Ω as shown in Fig. 2(b). Therefore, an orthogonal current mode can be obtained to eliminate the spatial coupling from Ant1 to Ant2. Furthermore, as shown in Fig. 2(c) and (d), the ground plane current has the same direction along the *x*-axis when fed through port 1, while the current direction is inverse when fed through port 2; hence, an orthogonal ground current mode is acquired which can block

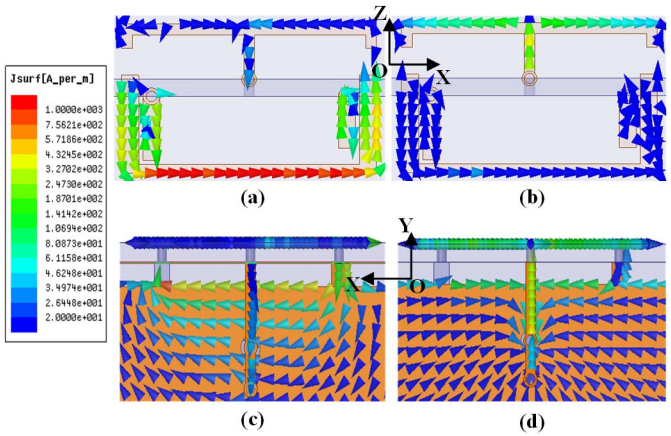

Fig. 2. Vector current distributions of the compact orthogonal-mode antenna pair and ground plane at 3.5 GHz. (a) Antenna pair current distribution fed through port 1 (dipole mode). (b) Antenna pair current distribution fed through port 2 (monopole mode). (c) Ground plane current distribution fed through port 1 (dipole mode). (d) Ground plane current distribution fed through port 2 (monopole mode).

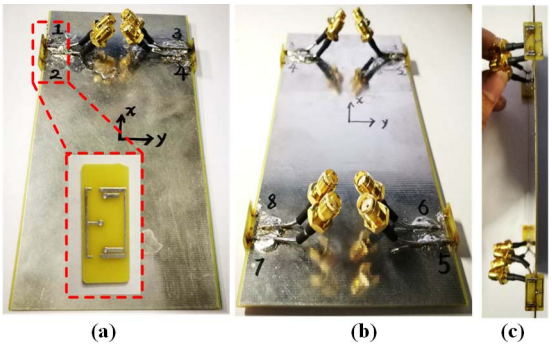

Fig. 3. Photographs of the proposed 4 × 4 and 8 × 8 MIMO systems. (a) Back view of the 4 × 4 MIMO system and the sideboard is enlarged in red dashed square. (b) Back view of the 8 × 8 MIMO system. (c) Side view of the 8 × 8 MIMO system.

the current coupling through the ground plane. In brief, a desirable decoupling performance of the tightly arranged dual antenna pair is obtained with the help of two sets of orthogonal modes: 1) the orthogonal current distribution of the dual antenna pair, hence, the spatial coupling can be mitigated and 2) the orthogonal current distribution on the ground plane, hence, the coupling through the ground current can also be blocked. Thus, a good isolation of better than 20 dB between Ant1 and Ant2 is achieved with the help of the orthogonal mode, which is different from [4]–[6] theoretically and the isolation is much better than that in [4]–[6].

C. S-Parameter

A prototype of the 4 × 4 MIMO system was fabricated to validate the S-parameter and radiation performance. The back view of the fabricated 4 × 4 MIMO system is shown in Fig. 3(a). Four 50 Ω semirigid cables were used to feed four ports of the MIMO system. Two sideboards are fixed along the left and right sides of the ground plane using the glue, and the enlarged view of the sideboard is shown in the red dashed square.

The measured and simulated reflection coefficients of the 4 × 4 MIMO system fed through ports 1 and 2 are depicted in Fig. 4, and the reflection coefficients of ports 3 and 4 are not given for brevity because they are completely symmetric with ports 1 and 2. A good agreement is obtained between the simulated and measured results and they are all better than −6 dB across the desired band.

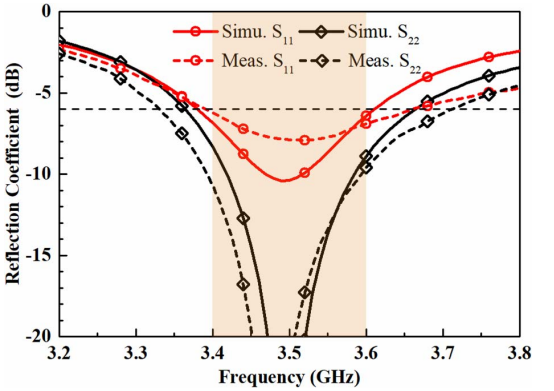

Fig. 4. Simulated and measured reflection coefficient of the 4 × 4 MIMO system.

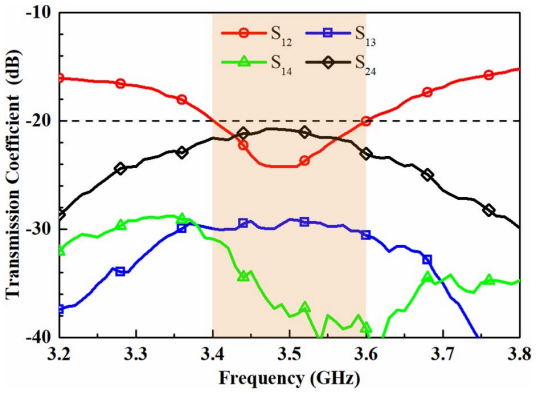

Fig. 5. Measured isolation of the 4 × 4 MIMO system.

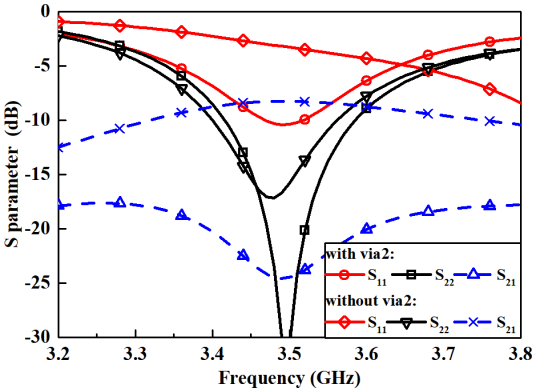

Fig. 6. Simulated S-parameter of the orthogonal-mode pair with or without via 2.

The bandwidth of Ant1 is less than Ant2 while the region occupied by Ant1 is larger than Ant2 because Ant1 with $\lambda/2$ resonance is close to the ground plane which will increase the Q-factor. The measured isolation of the 4 × 4 MIMO system is shown in Fig. 5, owing to the orthogonal mode of the elements, a high isolation performance of better than 20 dB across the desired band is acquired.

D. Parameter Analyzing

For the edge-fed dipole (Ant1), the grounded strip is an important structure to balance the current distribution on the right and left parts of the dipole and ground plane. If the balance of the current distribution is broken, the isolation between two orthogonal modes will decrease sharply. As shown in Fig. 6, if we remove via 2, which is a grounded point of Ant1, the impendence matching of Ant1 will be affected and the isolation between Ant1 and Ant2 decreases sharply from 20 to 8.2 dB. Fig. 7 shows the vector

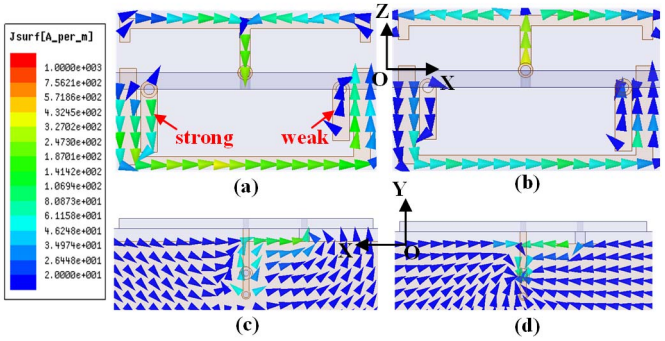

Fig. 7. Vector current distributions without via 2 at 3.5 GHz. (a) Antenna pair current distribution fed through port 1 (dipole mode). (b) Antenna pair current distribution fed through port 2 (monopole mode). (c) Ground plane current distribution fed through port 1 (dipole mode). (d) Ground plane current distribution fed through port 2 (monopole mode).

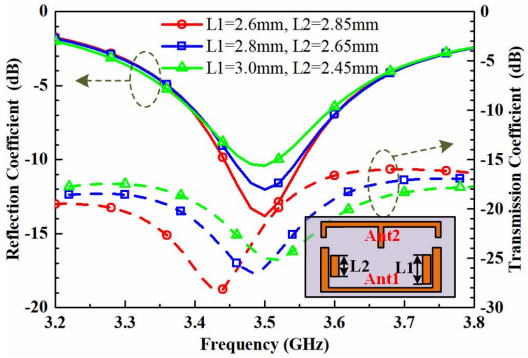

Fig. 8. Simulated reflection coefficient and transmission coefficient with different values of fed strip length L_1 and grounded strip length L_2.

current distributions of the proposed orthogonal-mode pair without the grounded point via 2. As shown in Fig. 7(a), when fed through port1, the current distribution in the left and right strips of Ant1 is unbalanced. Consequently, the current distribution in the ground plane is also unbalanced as shown in Fig. 7(c). Thus, the current mode between Ant1 and Ant2 is not orthogonal anymore. Strong current is coupled to Ant2 when Ant1 is exited and vice versa.

The lengths of fed strip L_1 and grounded strip L_2 are two significant parameters to balance the current mode and tuning the resonant frequency of Ant1. If we vary L_1 and L_2, respectively, S_{11} and S_{21} will be varied simultaneously. In order to avoid it, we let L_1 and L_2 vary simultaneously with the sum of L_1 and L_2 fixed, as shown in Fig. 8. The resonant frequency of Ant1 remains constant because the loading effect of the two strips is almost unchanged. However, the dip of S_{21} is shifted to a higher frequency with the difference of L_1 and L_2 increasing. Therefore, the dip of isolation can be controlled independently with the resonant frequency of Ant1 fixed; a good isolation can be obtained by optimizing the values of L_1 and L_2.

E. Radiation Pattern

Fig. 9 shows the radiation patterns of the proposed tightly arranged pair when fed through port 1 (dipole mode) and port 2 (monopole mode). As shown in Fig. 9(a) and (b), a dipolelike radiation pattern with a null point along the x-axis is obtained but the radiation pattern along the y- and z-axes is asymmetric because of the influence of the metal ground plane. The radiation pattern of the monopole shown in Fig. 9(c) and (d) is influenced by the ground plane because the ground plane is the dominant radiator for the monopole antenna. As shown in Fig. 9(a) and (c), the radiation patterns of

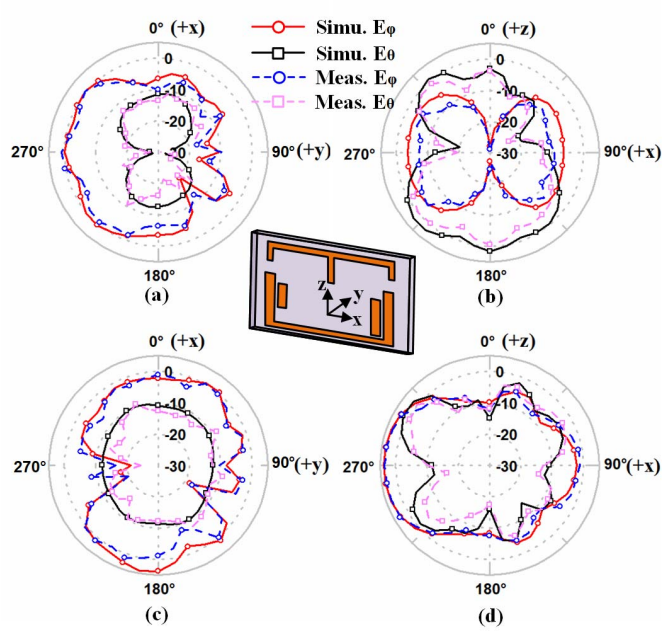

Fig. 9. Simulated and measured radiation patterns of the proposed tightly arranged pair at 3.5 GHz. (a) Port 1 in the *xy* plane. (b) Port 1 in the *xz* plane. (c) Port 2 in the *xy* plane. (d) Port 2 in the *xz* plane.

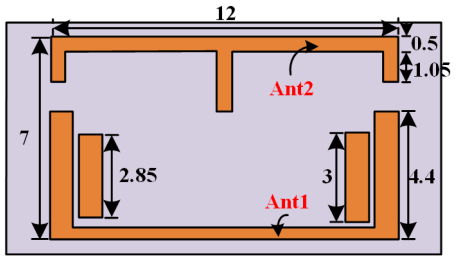

Fig. 10. Structure and detailed dimensions of the dual antenna pair of the 8 × 8 MIMO system, unit all in millimeters.

Ant1 and Ant2 toward the $-y$-direction are the maximum point and null point, respectively, and the same phenomenon can be observed in Fig. 9(b) and (d) along the $-z$-direction. Consequently, the radiation patterns of Ant1 and Ant2 are orthogonal with each other, thus, a low ECC can be obtained, which will be shown in Section IV.

III. Eight-Antenna MIMO System

A. Antenna Configuration of the 8 × 8 MIMO System

To enhance the channel capacity of the MIMO system, an 8 × 8 MIMO prototype was also fabricated to validate the extendibility of the aforementioned 4 × 4 MIMO system. The back view and side view of the fabricated MIMO system are shown in Fig. 3(b) and (c), respectively. Similar to the 4 × 4 MIMO system, eight 50 Ω semirigid cables were used to feed all ports of the MIMO system and four side edge boards are fixed along the left and right sides of the ground plane. It should be noted that L_d (illustrated in Fig. 1) is shorted from 30 to 25 mm for optimizing the isolation between every dual antenna pairs. Hence, the size of the 8 × 8 MIMO system is slightly different from the 4 × 4 MIMO system while the total size of a dual antenna pair is still 12 × 7 mm^2. The key parameters of the dual antenna pair of the 8 × 8 MIMO system are shown in Fig. 10, and other parameters that are identical to the 4 × 4 MIMO system are not given for brevity.

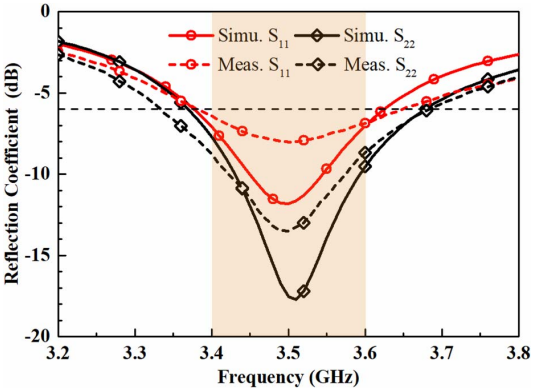

Fig. 11. Simulated and measured reflection coefficients of the 8 × 8 MIMO system.

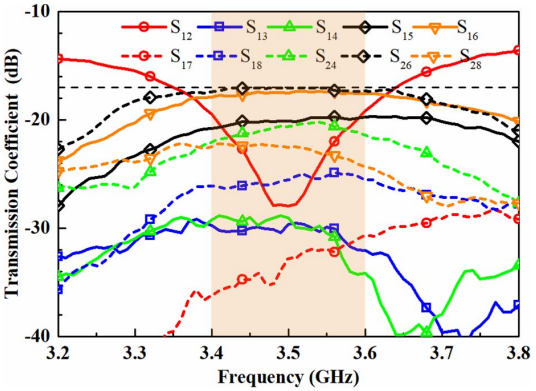

Fig. 12. Measured isolation of the 8 × 8 MIMO system.

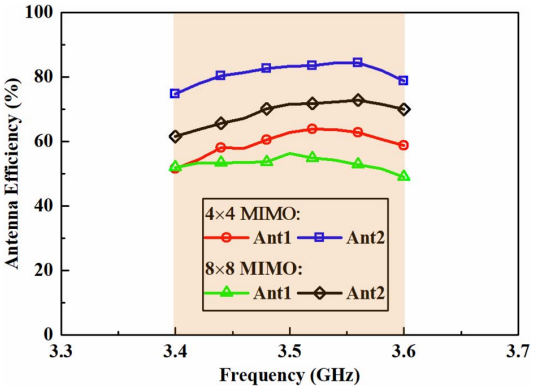

Fig. 13. Measured total antenna efficiencies of the 4 × 4 MIMO and 8 × 8 MIMO systems.

B. S-Parameter

Fig. 11 shows the measured and simulated reflection coefficients of the 8 × 8 MIMO system fed through ports 1 and 2 and the reflection coefficients fed through ports 3–8 are not given for brevity. The simulated and measured reflection coefficients are all better than −6 dB for the 8 × 8 MIMO system. The measured isolation of the 8×8 MIMO system is shown in Fig. 12, and the isolation performance is better than 17 dB for all ports, which is slightly worse than the 4 × 4 MIMO system for balancing the distances among every dual antenna pairs.

IV. Antenna Efficiency and Diversity Performance

A. Antenna Efficiency

The measured efficiencies of the proposed 4 × 4 MIMO system and 8 × 8 MIMO system fed through ports 1 and 2 are shown in Fig. 13. For the 4 × 4 MIMO system, good efficiencies of 51.7%–63.9% and

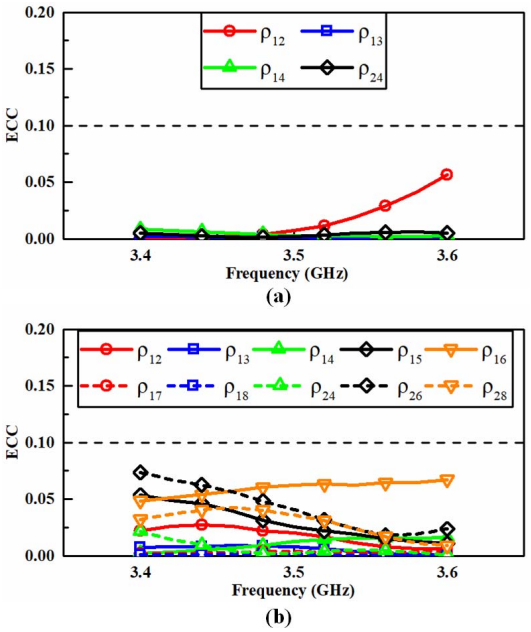

Fig. 14. Measured ECCs of the (a) 4×4 MIMO system and (b) 8×8 MIMO system.

TABLE I

COMPARISONS OF THE MIMO SYSTEM WITH COMPACT DUAL ANTENNA PAIR

Ref.	Dimension of a pair (mm^2)	Center Freq. (GHz)	Isolation	Effi.	ECC
[4][a]	19×3	3.5	>10dB	>40%	<0.25
[5]	10×7	3.5	>10dB	>40%	<0.1
[6]	15×7	3.5/5.8	>11dB	>50%	<0.15
[7]	20.6×20.6	2.6[b]	>12dB	>48%	<0.15
Proposed 4×4 MIMO	12×7	3.5	>20dB	>51%/ 74%	<0.06
Proposed 8×8 MIMO	12×7	3.5	>17dB	>49%/ 61%	<0.07

[a]only the results of 8×8 MIMO Array A in paper [4] is given because it has better performance than the other versions.

[b]the reflection coefficient is less than -10dB across the desired band in [14].

74.7%–84.5% are achieved when fed through ports 1 and 2. While for the 8×8 MIMO system, the antenna efficiency is 49%–56.4% and 61.6%–72.9% when fed through ports 1 and 2, which is slightly lower than the 4×4 MIMO system.

B. Diversity Performance

To quantitatively evaluate the diversity performance of the proposed MIMO system, the ECC is calculated by the complex radiation far field measured in an anechoic chamber. The measured ECCs of the 4×4 MIMO system and 8×8 MIMO system are illustrated in Fig. 14(a) and (b), respectively. The ECCs are less than 0.06/0.07 for the $4 \times 4/8 \times 8$ MIMO system within the desired band, which shows a promising diversity performance for a MIMO system. The good diversity performance is obtained due to the orthogonal radiation pattern and high port isolations.

C. Comparison

In addition, to make the merits of the proposed MIMO system explicit, a comparison chart is illustrated in Table I. From Table I,

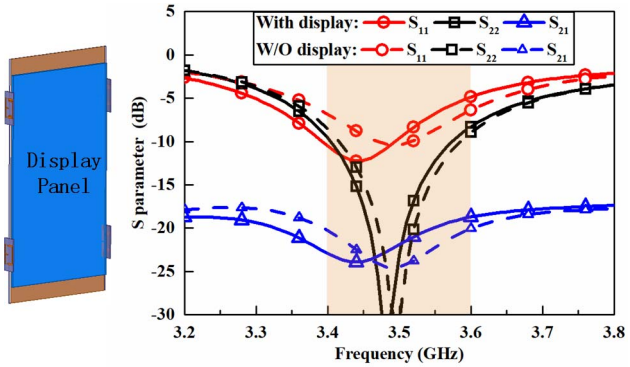

Fig. 15. Simulated S-parameter of the 8×8 MIMO system with and without display panel.

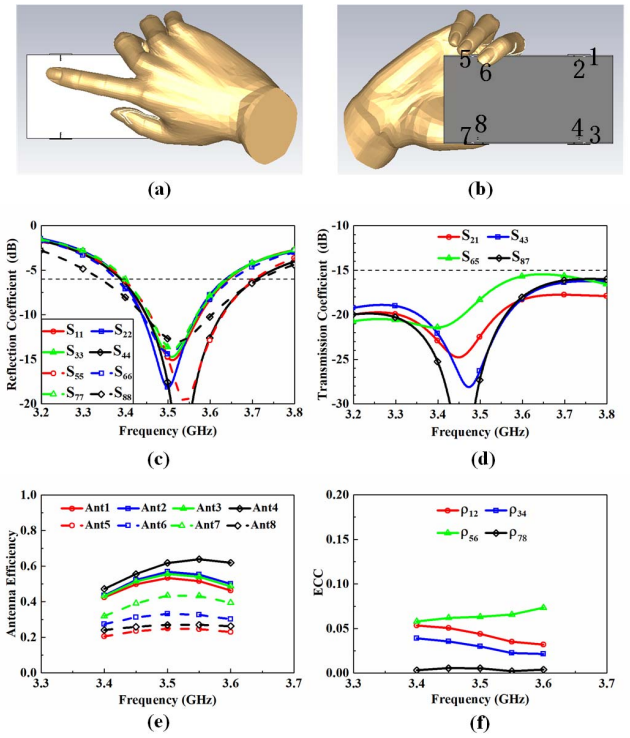

Fig. 16. Simulated results with user's hand of the proposed 8×8 MIMO system. (a) Front side of single-handhold scenario. (b) Back side of single-handhold scenario. (c) Reflection coefficient. (d) Transmission coefficient. (e) Antenna efficiency. (f) Envelope correlation coefficient.

we can draw the conclusion that an orthogonal-mode decoupling method is proposed to obtain better isolation and ECC performance than the existing works within a compact size. Although [5] has a more compact size with two quarter wavelength units, the isolation, efficiency, and ECC of this communication are all better than that in [5]. Besides, the decoupling mechanism of this communication is different from that in [5].

V. PRACTICAL APPLICATION DISCUSSION

A. Display Panel Effects

To study the influence of the display panel, a glass ($\varepsilon_r = 5.5$) with the size of $130 \times 73 \times 2$ mm^3 is added right above the ground plane and the spacing between the display panel and sideboards is 1 mm. The reflection coefficients and isolation with and without the display panel are illustrated in Fig. 15. S_{11} and S_{21} have small frequency shifts while S_{22} is almost unchanged. Owing to the display panel on the front side of the ground plane, it is near to Ant1 and far away from Ant2, so the frequency shift of Ant1 is more severe than Ant2.

The isolation is still better than 18 dB with the presence of the display panel because the orthogonal current mode is not broken. As a consequence, the proposed MIMO system is feasible in a practical environment.

B. User's Hand Effects

The effects of a user's hand for the proposed 8×8 MIMO system are shown in Fig. 16. Fig. 16(a) and (b) shows the typical single-handhold scenario of the user's hand. The corresponding simulated results within this hold scenario are shown in Fig. 16(c)–(f). The reflection coefficients are still better than -6dB for all of the elements with little frequency shifts as shown in Fig. 16(c). The isolations are better than 15 dB among all ports, and only the isolations between tightly coupled pairs are shown in Fig. 16(d) for the conciseness of the figure. The antenna efficiencies with the user's hand are shown in Fig. 16(e), and the efficiencies of Ant1–Ant4 have a little influence while the efficiencies of Ant5–Ant8 are declined because the user's hand is much close to them. The hand is lossy media that will absorb the radiant energy of antennas. However, the efficiencies are better than 20% for Ant5–Ant8. The ECCs have a little effect that is less than 0.075 as shown in Fig. 16(f) due to high isolations between every port.

VI. Conclusion

In this communication, a 4×4 MIMO system and an 8×8 MIMO system composed of compact tightly arranged pairs are presented. Good isolation and ECC performance are obtained owing to the orthogonal mode of the compact dual antenna pairs although the elements of the pair are closely spaced. This decoupling mechanism does not need any external structure, and the measured isolation is better than 20 dB/17 dB of the proposed $4 \times 4/8 \times 8$ MIMO system. Besides, the radiation efficiency of the proposed $4 \times 4/8 \times 8$ MIMO system is 51.7%–84.5%/49%–72.9%, and the ECCs of the proposed $4 \times 4/8 \times 8$ MIMO system are better than 0.06/0.07 across the entire band. In addition, some practical application with display panel effects and user's hand effects has been studied. The proposed MIMO systems provide a new solution to compact 5G MIMO mobile phone antennas with good isolation and diversity performance.

References

[1] I. Poole. (May 31, 2015). *LTE Frequency Bands and Spectrum Allocations*. [Online]. Available: http://www.radio-electronics.com/

[2] A. A. Al-Hadi, J. Ilvonen, R. Valkonen, and V. Viikari, "Eight-element antenna array for diversity and mimo mobile terminal in LTE 3500 MHz band," *Microw. Opt. Technol. Lett.*, vol. 56, no. 6, pp. 1323–1327, Jun. 2014.

[3] K.-L. Wong and J. Y. Lu, "3.6-GHz 10-antenna array for mimo operation in the smartphone," *Microw. Opt. Technol. Lett.*, vol. 57, no. 7, pp. 1699–1704, Jul. 2015.

[4] K. L. Wong, J.-Y. Lu, L.-Y. Chen, W.-Y. Li, and Y.-L. Ban, "8-antenna and 16-antenna arrays using the quad-antenna linear array as a building block for the 3.5-GHz LTE MIMO operation in the smartphone," *Microw. Opt. Technol. Lett.*, vol. 58, no. 1, pp. 174–181, Jan. 2016.

[5] K.-L. Wong, C.-Y. Tsai, and J.-Y. Lu, "Two asymmetrically mirrored gap-coupled loop antennas as a compact building block for eight-antenna MIMO array in the future smartphone," *IEEE Trans. Antennas Propag.*, vol. 65, no. 4, pp. 1765–1778, Apr. 2017.

[6] K.-L. Wong, B.-W. Lin, and W.-Y. Li, "Dual-band dual inverted-F/loop antennas as a compact decoupled building block for forming eight 3.5/5.8-GHz MIMO antennas in the future smartphone," *Microw. Opt. Technol. Lett.*, vol. 59, no. 11, pp. 2715–2721, Nov. 2017.

[7] M.-Y. Li, Z.-Q. Xu, Y.-L. Ban, C.-Y.-D. Sim, and Z.-F. Yu, "Eight-port orthogonally dual-polarised MIMO antennas using loop structures for 5G smartphone," *IET Microw. Antennas Propag.*, vol. 11, no. 12, pp. 1810–1816, Sep. 2017.

[8] L. Sun, H. Feng, Y. Li, and Z. Zhang, "Tightly arranged orthogonal mode antenna for 5G MIMO mobile terminal," *Microw. Opt. Technol. Lett.*, vol. 60, no. 7, pp. 1751–1756, Jul. 2018.

[9] X. Shi, M. Zhang, S. Xu, D. Liu, H. Wen, and J. Wang, "Dual-band 8-element MIMO antenna with short neutral line for 5G Mobile Handset," in *Proc. 11th Eur. Conf. Antennas Propag. (EUCAP)*, Mar. 2017, pp. 3140–3142.

[10] M.-Y. Li *et al.*, "Eight-port orthogonally dual-polarized antenna array for 5G smartphone applications," *IEEE Trans. Antennas Propag.*, vol. 64, no. 9, pp. 3820–3830, Sep. 2016.

[11] H. Xu, H. Zhou, S. Gao, H. Wang, and Y. Cheng, "Multimode decoupling technique with independent tuning characteristic for mobile terminals," *IEEE Trans. Antennas Propag.*, vol. 65, no. 12, pp. 6739–6751, Dec. 2017.

[12] A. F. Molisch and M. Z. Win, "MIMO systems with antenna selection," *IEEE Microw. Mag.*, vol. 5, no. 1, pp. 46–56, Mar. 2004.

[13] A. Diallo, C. Luxey, P. L. Thuc, R. Staraj, and G. Kossiavas, "Study and reduction of the mutual coupling between two mobile phone PIFAs operating in the DCS1800 and UMTS bands," *IEEE Trans. Antennas Propag.*, vol. 54, no. 11, pp. 3063–3074, Nov. 2006.

[14] Y. Wang and Z. Du, "A wideband printed dual-antenna system with a novel neutralization line for mobile terminals," *IEEE Antennas Wireless Propag. Lett.*, vol. 12, pp. 1428–1431, 2013.

[15] A. C. K. Mak, C. R. Rowell, and R. D. Murch, "Isolation enhancement between two closely packed antennas," *IEEE Trans. Antennas Propag.*, vol. 56, no. 11, pp. 3411–3419, Nov. 2008.

[16] S. Zhang, B. K. Lau, Y. Tan, Z. Ying, and S. He, "Mutual coupling reduction of two PIFAs with a T-shape slot impedance transformer for MIMO mobile terminals," *IEEE Trans. Antennas Propag.*, vol. 60, no. 3, pp. 1521–1531, Mar. 2012.

[17] C.-Y. Chiu, C.-H. Cheng, R. D. Murch, and C. R. Rowell, "Reduction of mutual coupling between closely-packed antenna elements," *IEEE Trans. Antennas Propag.*, vol. 55, no. 6, pp. 1732–1738, Jun. 2007.

[18] S. C. Chen, Y. S. Wang, and S. J. Chung, "A decoupling technique for increasing the port isolation between two strongly coupled antennas," *IEEE Trans. Antennas Propag.*, vol. 56, no. 12, pp. 3650–3658, Dec. 2008.

[19] Y. Li, Z. Zhang, W. Chen, Z. Feng, and M. F. Iskander, "A dual-polarization slot antenna using a compact CPW feeding structure," *IEEE Antennas Wireless Propag. Lett.*, vol. 9, pp. 191–194, 2010.

[20] Y. Li, Z. Zhang, J. Zheng, and Z. Feng, "Compact azimuthal omnidirectional dual-polarized antenna using highly isolated colocated slots," *IEEE Trans. Antennas Propag.*, vol. 60, no. 9, pp. 4037–4045, Sep. 2012.

[21] J. Zhu and G. V. Eleftheriades, "A simple approach for reducing mutual coupling in two closely spaced metamaterial-inspired monopole antennas," *IEEE Antennas Wireless Propag. Lett.*, vol. 9, pp. 379–382, 2010.

[22] Z. Zhang, *Antenna Design for Mobile Devices*, 2nd ed. Hoboken, NJ, USA: Wiley, 2017.

[23] K.-L. Wong, *Compact and Broadband Microstrip Antennas*. New York, NY, USA: Wiley, 2012.